Field data confirm the ability of a biophysical model to predict wild primate body temperature

Paul D. Mathewson[a], Warren P. Porter[a], Louise Barrett[b,c], Andrea Fuller[c], S. Peter Henzi[b,c], Robyn S. Hetem[c,d], Christopher Young[b,e,f], Richard McFarland[a,c,g]

[a] Department of Integrative Biology, University of Wisconsin–Madison, USA.

[b] Department of Psychology, University of Lethbridge, Canada

[c] Brain Function Research Group, School of Physiology, Faculty of Health Science, University of the Witwatersrand, South Africa.

[d] School of Animal, Plant and Environmental Sciences, Faculty of Science, University of the Witwatersrand, South Africa.

[e] Applied Behavioural Ecology & Ecosystems Research Unit, University of South Africa, South Africa

[f] Endocrine Research Laboratory, Mammal Research Institute, Faculty of Natural and Agricultural Science, University of Pretoria, Pretoria, South Africa

[g] Department of Anthropology, University of Wisconsin–Madison, USA.

Corresponding Author: Paul D. Mathewson

Department of Integrative Biology, University of Wisconsin, Madison

250 North Mills Street, Madison, WI 53706

Email: mathewson@wisc.edu

ABSTRACT

In the face of climate change there is an urgent need to understand how animal performance is affected by environmental conditions. Biophysical models that use principles of heat and mass transfer can be used to explore how an animal's morphology, physiology, and behavior interact with its environment in terms of energy, mass and water balances to affect fitness and performance. We used Niche Mapper™ (NM) to build a vervet monkey (*Chlorocebus pygerythrus*) biophysical model and tested the model's ability to predict core body temperature (T_b) variation and thermal stress against T_b and behavioral data collected from wild vervets in South Africa. The mean observed T_b in both males and females was within 0.5°C of NM's predicted T_bs for 91% of hours over the five-year study period. This is the first time that NM's T_b predictions have been validated against field data from a wild endotherm. Overall, these results provide confidence that NM can accurately predict thermal stress and can be used to provide insight into the thermoregulatory consequences of morphological (e.g., body size, shape, fur depth), physiological (e.g. T_b plasticity) and behavioral (e.g., huddling, resting, shade seeking) adaptations. Such an approach allows users to test hypotheses about how animals adapt to thermoregulatory challenges and make informed predictions about potential responses to environmental change such as climate change or habitat conversion. Importantly, NM's animal submodel is a general model that can be adapted to other species, requiring only basic information on an animal's morphology, physiology and behavior.

KEY WORDS

Chlorocebus pygerythrus; ecological energetics; endotherm; metabolic rate; Niche Mapper; thermoregulation; vervet monkey

1. INTRODUCTION

Given the threat that global climate change poses to biodiversity (Pacifici et al. 2015, Urban et al. 2016) there is a pressing need to understand the fitness consequences of environmental changes from a physiological perspective (Fuller 2010). Endotherms employ a range of adaptations to cope with environmental challenges, and when unable to maintain their optimal body temperature range, animals can experience reduced cellular efficiency and fitness (Seebacher and Little 2017, Maloney et al. 2017). Homeothermy – maintaining a body temperature within a relatively narrow range despite environmental temperature variation – is achieved through a combination of physiological (autonomic) and behavioral processes. Physiological processes can be costly in terms of energy expenditure through increased metabolic heat production and water loss through evaporative cooling (Fuller et al. 2016, Levesque et al. 2016). To reduce the physiological costs of thermoregulation, individuals can also engage in behaviors that influence heat exchange with the environment, including changing activity patterns, postural adjustments or selecting thermally-advantageous microclimates (Speakman and Krol 2010, Huey et al. 2012, McFarland et al. 2015, Mason et al. 2017, McFarland et al. 2019, 2020). Behavioral thermoregulation, however, may take place at the expense of other behaviors critical to survival (e.g., feeding, drinking, traveling, and social activity; McFarland et al. 2014, Dunbar et al. 2009).

Thermoregulatory mechanisms require time and resources that could otherwise be used for growth and reproduction. Therefore, fitness-related activities are essentially traded and prioritized according to social, ecological, and environmental factors. The fundamental challenge for an endotherm is to balance these activities—and their associated costs—without operating in a long-term negative energy or water balance. Species distributions are thought to be determined

by sublethal impacts of thermal stress on performance rather than physiological thresholds for direct temperature-related mortality (Buckley et al. 2012, Evans et al. 2015). Thus, being able to predict consequences of thermal stress can provide valuable insight into understanding current distributions and potential responses to climate change.

The most common approach to modeling species' distributions involves statistically relating a species' occurrence locations with environmental predictors such as climate and land cover (Elith and Leathwick 2009). The resulting *n*-dimensional space that represents the range of environmental conditions at known presence locations is considered the animal's bioclimatic "envelope". These envelopes are then projected onto future climate scenarios to predict changes in distribution (Hijmans and Graham 2006). Taking a correlative approach to distribution modeling, however, provides little insight into how environmental predictors limit distributions, since the limiting processes remain implicit in the correlations (Dormann et al, 2012, Evans et al. 2015). Correlative approaches also require extrapolation into novel environments, such as those created by climate change, increasing the risk of erroneous predictions (Buckley and Kingsolver 2012, Pacifici et al. 2015). In contrast, mechanistic models explicitly model the processes thought to limit a species' distribution. By explicitly modeling the processes, predicted distributions are based entirely on the model's predictions of where survival is possible, independent of observed distributions. Mechanistic models are therefore more informative than correlative models and can be applied to novel conditions without extrapolation (for comprehensive comparisons of correlative and mechanistic approaches, see Kearney and Porter 2009, Buckley et al. 2010).

One mechanistic approach to understanding distributional limits is the use of biophysical models, which are based on fundamental principles of heat and mass transfer, and model how an

animal's morphology, physiology, and behavior interact with its environment in terms of energy, dry mass and water balances to affect fitness and performance (Porter and Gates 1969; Kearney and Porter 2009). A biophysical model can thus be used to quantify thermal stresses incurred by an animal in any environment. These stresses include increased heat production and food requirements in response to cold stress, and increased evaporative water loss and/or reduced activity in response to heat stress. This quantification provides insight into how a species' distribution is limited by environmental temperatures (Kearney and Porter 2009). In the context of climate change, biophysical models can be used to investigate the direct impact of higher environmental temperatures on an animal's thermal performance and habitat suitability across the landscape. By modeling these consequences mechanistically, taking an animal's specific characteristics into account, biophysical models can be used to examine how intraspecific variation in morphological and physiological traits, as well as behavioral responses, might allow a species to buffer the impacts of climate stress.

Here, we build and test a vervet monkey (*Chlorocebus pygerythrus*) model with Niche Mapper (Porter and Mitchell 2006; hereafter, 'NM'), a biophysical modeling software package. Local climates impose an important ecological constraint on primate distributions (Korstjens et al. 2010, Lehmann et al. 2010), so understanding how primates respond to changes in the thermal environment is essential if we are to assess how climate change will impact species survival in a taxon that is already facing substantial pressure (Estrada et al. 2017). NM has been used to accurately predict the energetic requirements and thermal stress as a function of environmental conditions for a wide variety of animals, including the following mammals: American pika (*Ochotona princeps*; Moyer-Horner et al. 2015), Japanese serow (*Capricornus crispus*; Natori and Porter 2007), giant panda (*Ailuropoda melanoleuca*; Zhang et al. 2018), elk (*Cervus elaphus*;

Long et al 2014), polar bear (*Ursus maritimus;* Mathewson and Porter 2013), and koala (*Phascolarctos cinereus*; Briscoe et al. 2016). However, to date no study has validated whether NM accurately predicts body temperatures (T_b) in wild endotherms. T_b is a key driver of NM's calculations and thus validation of accurate T_b predictions will provide increased confidence in NM's ability to accurately predict energetic requirements and thermal stress in wild environments.

We aim to provide the first test of NM's ability to predict core body temperatures (T_b) of a wild endotherm, the vervet monkey (*Chlorocebus pygerythrus*). Using a combination of direct measurements and information obtained from existing literature, we parameterize a vervet biophysical model. We first assess the vervet model in the controlled environment of a simulated metabolic chamber by evaluating whether the model predicts a reasonable thermoneutral zone. Next, we perform a series of sensitivity analyses to illustrate which morphological, physiological and behavioral inputs have the biggest impact on the model's predictions of thermoneutral zone, metabolic heat production, and T_b. Finally, using a set of models parameterized to bracket the range of behaviors observed in a wild population of vervets, we use NM to make T_b predictions, and will compare those predictions to measurements taken *in situ* from the wild population. Given our multiyear dataset on the T_b, behavior, and local climate of a wild population, we are uniquely positioned to test NM's ability to predict a wild endotherm's thermal response to the environment. Vervets represent an excellent model to meet this objective, as they experience a wide temperature range in varied environments (Pasternak et al. 2012; McFarland et al. 2014), and possess a range of behavioral and thermoregulatory adaptations (McFarland et al. 2015, 2019, 2020).

2. METHODS

2.1 Study site, subjects, and wild animal data collection

Between 2012 and 2016, we collected field data from a population of wild vervet monkeys living on the Samara Private Game Reserve in the Eastern Cape, South Africa (32°22'S, 24°52'E). We recorded local climate at an onsite weather station (McFarland et al. 2015). This semi-arid region has a seasonal climate, with hot, wet summers, and cold, dry winters. Annual rainfall is < 400mm, while minimum and maximum air temperatures typically range between -5 and 40ºC (McFarland et al. 2014).

As part of a long-term study of vervet monkey thermal physiology, we abdominally implanted 45 vervets with body temperature data loggers that recorded core T_b at five-minute intervals (mean = 16.4 ± 10.6 months/monkey; Table A.1). Vervets were immobilized using blow darts filled with a combination of midazolam and ketamine, and following recumbence, were transported to a temporary operating theatre where they were weighed. A qualified veterinarian administered the appropriate analgesic, anti-inflammatory and antibiotic medication, and followed standard, ethically-approved, aseptic surgical techniques for the implantation of data loggers. The vervets were allowed to recover fully in cages before being released back into their group. Normal behavior resumed on the day after surgery, and no long-term sequelae were observed as a consequence of surgical intervention, as confirmed by regular behavioral monitoring by researchers and a veterinarian. See McFarland et al. (2015) for full details of the implantation procedure. Since NM performs energy balance calculations on an hourly basis (see section 2.2 below), we calculated the average hourly T_bs for male and female monkeys from the five-minute observational data, allowing us to directly compare observed T_b and NM's predicted T_b. Vervet 24-hour T_b patterns follow a square wave pattern with lower and upper modal T_bs

(Lubbe et al. 2014). The lower modal T_b for the current study animals (based on 479,530 individual vervet hour T_b measurements) was 37.1°C and the upper modal T_b was 38.6°C (Fig. A.1a). The modal T_bs were similar between sexes and across seasons (Fig. A.1b).

We collected detailed morphometric data from four males and two females (2015) and two males (2016) during their respective animal captures. In 2015, we used a tape measure to measure the length and width of each animal's head, torso, arms, legs and tails. In 2016, we used calipers to measure the fur depth and hair length on each of these same body parts, allowing us to calculate the hair length:fur depth ratios for two subjects. We used vervet pelt reflectance values measured by McFarland et al. (2016), where trapezoidal integration of each wavelength interval (5nm between 250-3500nm) was scaled according to the solar energy in that interval to calculate overall solar reflectivity. We measured hair diameter and density from two pelts (McFarland et al. 2016) using an ocular calibration grid and micrometer with a light microscope.

All capture and surgical procedures were approved by the University of the Witwatersrand Animal Ethics Research Committee (Protocols # 2010/41/04 and 2015/04/14B), and all animals were treated in accordance with international ethical standards. Importantly, vervets were not exposed to the above surgical procedures for the purpose of the current project. These T_b data were collected as part of a longitudinal study of vervet monkey thermal physiology (see, e.g., Lubbe et al. 2012; McFarland et al. 2015, 2019, 2020; Henzi et al. 2017) and body temperature data collected during the study were opportunistically utilized for the current study.

2.2 Modelling Methodology

2.2.1 Niche Mapper - General Description

NM consists of a microclimate submodel and an animal submodel (Fig. 1). The microclimate submodel uses hourly interpolation of macroclimate data (maximum and minimum daily air temperatures, relative humidity, cloud cover, and wind speed), and substrate properties, vegetative cover, geographic location, topography, and time of year to calculate hourly environmental profiles from 2m height down to the ground surface using numerical integration of a one-dimensional finite difference equation in the vertical dimension. The microclimate submodel also calculates sky temperatures and incoming solar radiation incident on the ground that is available for absorption by the model animal. Separate environmental profiles are calculated for full sun and shaded microenvironments (see Fuentes and Porter 2013 for more details on the microclimate model calculations).

The animal submodel uses morphological, physiological and behavioral information about the animal along with hourly microclimate submodel outputs (Fig. 1) to iteratively solve coupled heat and mass balance equations (Porter 2016) to find the metabolic rate needed for the animal to maintain its T_b, accounting for convective, radiative, evaporative and solar heat fluxes with its microenvironment for each hour of the day (see Mathewson and Porter 2013 for details on the heat balance calculations). Animal body parts are modelled as simple shapes (cones, cylinders, ellipsoids, spheres) with well-understood heat transfer properties that enable surface temperatures to be calculated based on a given T_b and body part dimensions. NM models heat flowing from the core to the skin surface, assuming distributed metabolic heat generation throughout the flesh of each body part. For bare body parts, heat fluxes with the environment are computed using the calculated skin surface temperatures. For furred body parts, heat is modeled as traveling through a porous fur layer composed of a matrix of air and keratin via parallel

conduction and radiative processes before heat exchange with the environment is calculated (Conley & Porter 1986).

NM solves the animal's heat balance for each hour of the day. Calculations for each hour begin by computing the metabolic heat production required for the animal to maintain its starting T_b (specified by the user, typically an average T_b;) in that hour's environmental conditions. Other parameters that are allowed to be modified for thermoregulatory purposes (Fig. 1) also begin each hour's calculations at their specified starting value. Thermoregulatory options are engaged if the required metabolic rate is above or below that hour's target metabolic rate. Target metabolic rates are either resting metabolic rate (during hours when animals are assumed to be inactive) or a multiple of resting metabolic rate to simulate activity (during hours when animals are assumed to be active). The user specifies whether the model animal is active or inactive separately for diurnal, crepuscular, and nocturnal hours. Users can supply a species-specific resting metabolic rate if data are available; otherwise the model estimates resting metabolic rate using a generic mammalian regression equation based on animal mass (Gordon et al. 1972).

Behavioral thermoregulatory options of selecting a different microhabitat (e.g., shade seeking in the heat) or changing posture (e.g., curling/huddling up in the cold) are engaged first, followed by physiological options. To minimize metabolic heat production above the target range in cold environmental conditions, animals are allowed to increase pelage depth (to simulate piloerection), decrease flesh thermal conductivity (to simulate vasoconstriction) and reduce T_b. To maintain a metabolic rate in a hot environment, animals are allowed to increase thermal conductivity (to simulate vasodilation), increase T_b, and increase surface area that is wet (simulating sweating). Thermoregulation will proceed until a heat balance is reached with a metabolic rate within the target range or until the model has reached the maximum or minimum

value for the thermoregulatory options (e.g., the maximum or minimum T_b allowed by the user). If thermoregulatory options are exhausted before a metabolic rate within the user-specified tolerable error (here, ±2.5%) of the target metabolic rate is reached, the model will return the metabolic rate closest to the target value that satisfies the heat balance.

2.2.2 Vervet Animal Model Parameterization

Using the morphometric data described above, we modeled vervets with ellipsoids for the head and cylinders for all other body parts. Our over-arching objective is to validate NM's ability to make accurate predictions of T_b. We use data collected from wild vervets to specify the model's starting (i.e., average: 38°C), minimum (36°C) and maximum (41°C) allowable T_b. These minimum and maximum T_b values are outside the bimodal distribution (37-39°C) of body temperature observed in this species. Although the starting temperature we define will be the starting point for NM's calculation of hourly heat balance, NM's final T_b prediction is the value that allows the animal to reach an acceptable heat balance in those conditions; ranging anywhere between the specified minimum and maximum T_b values. As part of its thermoregulatory loop, NM can adjust T_b in 0.1°C increments in order to reach an acceptable heat balance (Fig. 1). Thus, any variation in predicted T_b from the user-supplied starting T_b is due to the model predicting that a T_b change is needed to either maintain the target metabolic rate (T_b increase) or avoid additional metabolic heat production (T_b decrease) in that hour's environmental conditions. Daily T_b cycling is not programmed into the model. Any predicted T_b cycling is an emergent property of the hourly environmental conditions interacting with the animal model's morphological, physiological, and behavioral traits.

2.2.3 Thermoneutral Zone (TNZ) Predictions

Our first objective is an initial evaluation of model performance, investigating whether the environmental temperatures at which the male and female vervets models, parameterized as described above in section 2.2.3 to be used in the wild vervet T_b validations, predicts heat or cold stress (i.e., the upper and lower bound of its predicted TNZ) are reasonable. We define the upper critical temperature as the air temperature at which model vervets would not be able to maintain their resting metabolic rate without sweating (*sensu* Mitchell et al. 2018). We define the lower critical temperature as the air temperature at which model vervets would need to raise their metabolic heat production above the resting rate to maintain their T_b. In a real-world setting, air temperatures combine with ground and sky radiant temperatures, wind, humidity and solar radiation to create the effective temperature that the animal experiences. To identify the predicted upper and lower critical temperatures (i.e., the TNZ boundaries) more clearly, we placed the model animal into a simulated metabolic chamber in which all temperatures (i.e., air, ground, and sky) were set to the same value and then increased in 1°C increments, with no solar radiation, relative humidity set to 5%, and wind speeds set to 0.1m s^{-1}. Given our definition of upper critical temperature, the model vervets were not able to sweat in the metabolic chamber for the purpose of identifying the predicted thermoneutral zone, since sweating would indicate that it was already outside the TNZ. For the purposes of the TNZ analysis, we held the T_b constant at 38°C. All other morphological and physiological inputs were as listed in Table 1. Because experimental studies reporting TNZs rarely report the posture of the animal during the measurements, we simulated vervets in both a curled posture (simulated by combining the arms, legs, and torso into a single body part shape for the purposes of modeling heat exchange) and uncurled posture (all body parts available for heat exchange).

2.2.4 Sensitivity analyses

Our second objective is to perform a sensitivity analysis of the vervet model's biophysical inputs to examine which inputs have the greatest effect on the NM's thermal stress predictions for the vervets. Relevant morphological and physiological NM input values (pelage properties, body part dimensions, body size, resting metabolic rate, T_b variability) were adjusted from the value listed in Table 1 to assess how they affected the model's predicted upper and lower critical temperatures and whole-body thermal conductivity. Whole-body thermal conductivity was calculated as the slope of the predicted metabolic rate as a function of air temperature below the lower critical temperature (W °C^{-1}). All analyses were conducted in a simulated metabolic chamber, as described in section 2.2.3 with vervets being simulated as being uncurled (i.e., standing with hands and feet on the ground). For all sensitivity analyses except the T_b variability analysis, we held the T_b constant at 38°C.

With three exceptions, when one parameter was being analyzed, all other inputs remained at their user-supplied values listed in Table 1. First, when analyzing the effect of body size, the radial and linear dimensions of the body parts were scaled up or down proportionally to ensure the same body part proportions and densities. Second, when analyzing the effect of body part linear dimensions, body part radial dimensions were automatically adjusted in or out to ensure constant body part density (e.g., increasing linear dimensions would result in longer, thinner body parts). Third, when analyzing the effect of allowable T_b fluctuation, minimum and maximum T_b were set at either ± 0, 1, 2, or 3°C from the 38°C starting point.

2.2.5 Testing Niche Mapper's Ability to Predict Body Temperature in Wild Vervets

We simulated wild vervets for the data collection period (2012-2016) and compared T_b predictions to observed T_b from the wild vervet study population. These simulations allowed us to test NM's ability to accurately predict T_b and identify thermally stressful conditions. We used hourly temperatures recorded at the on-site weather station (placed in an unshaded location: see Lubbe et al. 2014 for details) to parameterize the microclimate model. Other microclimate model inputs are summarized in Table A.3. To bound potential microclimate conditions, we calculated microclimate conditions at animal height in the full sun (the hottest microclimate conditions) and in the full shade, with the ability to climb to a height where 2m climate conditions prevail (i.e., the coolest microclimate conditions).

NM models will always thermoregulate to minimize deviations from the target metabolic rate (i.e., resting or active) and will behaviorally thermoregulate before physiologically thermoregulating, thereby minimizing variation in T_b changes from the starting T_b. Thus, user choice of allowable thermoregulatory options will affect T_b predictions. For example, if vervets were allowed to seek shade and assume any nighttime posture, NM would immediately attempt to seek shade when the animal is first heat stressed during the day and start to huddle when first cold stressed at night before changing its T_b. Furthermore, during any diurnal hour, NM will always assume the vervet is active unless it is unable to maintain a heat balance at the active metabolic rate.

A real animal may behave in ways that affect metabolic rate and T_b for reasons unrelated to thermal stress. Therefore, a single set of model assumptions in terms of habitat choice, activity level, and posture is not universally applicable, and it would be inappropriate to evaluate NM's performance using a single set of model assumptions. Thus, we performed the wild vervet simulations with a cold animal model and a hot animal model in order to bracket possible

predicted T_bs. We parameterized the cold model to provide the lowest predicted T_b for any given hour. For diurnal hours the cold model was assumed to be inactive (i.e., targeting resting metabolic rate) with access to shade and the ability to climb to a cooler temperature above the ground. During nocturnal hours, the cold model was only allowed to use the least heat-conserving, "stretched" posture, which models all body parts exposed for heat exchange (representing a solitary individual draped across a branch). We parameterized the hot model to provide the highest predicted T_b for any given hour. During diurnal hours the hot model was assumed to be active with no access to shade or ability to climb to reach cooler temperatures. For each day within a given month we used the same activity multiplier as the active metabolic rate, with monthly multipliers varying from a low of 2.25x resting metabolic rate (RMR) in the summer to a maximum of 4.5x RMR in the winter. These multipliers were derived through a calibration process to obtain the closest fit between predicted and observed T_b for the 2012-2013 field season simulations and correspond to a 24-hour field metabolic rate of 1.75x RMR in the summer and 2.46x RMR in the winter when accounting for seasonal differences in day lengths. This activity variation is consistent with observations of higher activity in the colder months (McFarland et al. 2014; see also Cantaloup et al. 2019).

During nocturnal hours the hot model was allowed to use the most heat-conservative nocturnal body posture of huddling between other monkeys. Huddling was simulated by lumping multiple individuals together to reduce surface area available for heat exchange with the environment (Mathewson 2018) and is thought to be an important form of behavioral thermoregulation for vervets to minimize metabolic heat production overnight (McFarland et al. 2015). We assumed a warm huddling scenario to provide an upper bound of predicted nighttime T_b: a vervet in between two other individuals with 75% of its torso in contact with neighbors.

Other than the differences in behavioral parameters described above, the hot and cold models were parametrized identically (Table 1). For nocturnal hours (i.e., when the sun is below the horizon), the monkeys were simulated in both the hot and cold models as being inactive in a tree, where 2-m climate conditions determine the relevant microclimate. In both the hot and cold models, piloerection (allowing fur depth to increase to 50% of hair length), vasodilation/vasoconstriction, sweating (allowing up to 75% of the body to be covered in sweat for evaporative water loss), and T_b changes between the specified maximum and minimums were all allowed for thermoregulation.

To evaluate the importance of shade access (McFarland et al. 2020), we ran an additional simulation where we modified the cold model to not allow the model to seek shade during diurnal hours. To evaluate the importance of huddling and overnight posture (McFarland et al. 2015; Henzi et al 2017), we ran a final simulation where we modified the hot model so rather than huddling, it could only curl up at night. Curling up was simulated by combining the arms, legs, and torso into a single body part shape for the purposes of modeling heat exchange (representing a vervet curling its arms and legs into its torso).

We compared the mean observed T_b for each hour to the maximum and minimum predicted T_bs and the average of the maximum and minimum predicted T_b. We also evaluated how well NM's bracketed range of predicted T_bs captured the observed T_bs by calculating the number of hours that the mean observed T_b for each sex was between the minimum and maximum predicted T_b. Unless specifically noted when evaluating the importance of shade access or huddling, the maximum T_bs are from the hot model that allows huddling and the cold minimum T_bs are from the cold model that allows access to shade.

Finally, we calculated several daily metrics with both the observed and predicted T_b data: minimum T_b, maximum T_b, mean T_b, and 24-hour amplitude of T_b rhythm (difference between maximum and minimum T_b). For the observed data, we calculated these metrics based on hourly average T_bs for each sex, with the exception of 24-hour amplitude where individual amplitudes were calculated and an average for each sex was computed. For the predicted data, we calculated the ranges for each metric using the maximum and minimum T_b predictions from the hot model that allows huddling and the cold model that allows access to shade.

3. RESULTS

3.1 Thermoneutral Zone Prediction

The predicted thermoneutral zone (TNZ) for the model vervets ranged from 18°C (males) and 19°C (females) to 28°C (both sexes) without any postural change (Fig. A.3). Allowing a heat-conserving "curled" posture with arms and legs tucked into the torso reduced the lower critical temperature to 6°C (males) and 10°C (females) (Fig. A.3).

3.2 Sensitivity analyses

NM was most sensitive to changes in assumed resting metabolic rate, fur depth, the hair length:fur depth ratio, body part length:width ratio and allowable T_b range (Table 2; Figs. A.4-A.7). Increasing resting metabolic rate or any of the pelage inputs shifted the TNZ to lower temperatures, while increasing body part length:width ratio shifted the TNZ to higher temperatures. Upper and lower critical temperatures increased and decreased, respectively, by 1-2°C for each degree the T_b was able to vary from 38°C (Fig. A.7). The model was least sensitive to changes in hair diameter and density, although halving these values from the value used in the vervet model had a large effect on predicted critical temperatures (Fig. A.4).

3.3 Testing Niche Mapper's Ability to Predict Body Temperature

Examples of NM's maximum T_b (active in the sun during diurnal hours; inactive and huddled during crepuscular and nocturnal hours) and minimum predicted T_b (resting in the shade during diurnal hours; inactive and uncurled alone during crepuscular and nocturnal) along with the range of observed T_b for a hot and cold month are shown in Figure 2.

3.3.1 Diurnal Hours

NM's maximum, minimum and average (of the maximum and minimum, representing a mix of activity and shade use within the group) predicted T_bs during diurnal hours were compared to observed T_bs (Fig. 3). The minimum predicted T_b was typically lower than the observed T_b, while the maximum T_b prediction typically overestimated T_b compared to observed T_b. The average predicted T_b clustered around the observed upper modal T_b. NM's T_b predictions were also compared with observed T_b for each hour of the day across each season (Fig. 4). For most hours, the average predicted T_b was close to observed T_b (see also Fig. A.8 showing how the average predicted T_b clustered around the upper modal T_b), there were times when the average predicted T_b over- or under-predicted the observed T_b by more than 1°C (5.8% of hours for females; 8.3% of hours for males). During the earliest diurnal hours, NM over-predicts T_b if any activity was assumed (e.g., average and maximum T_b predictions for hours 04:00-05:00 in Fig. 4). For other hours, most of the over-predictions occur in the warmer months during the warmest hours of the day when the minimum NM prediction (a resting vervet) were closest to the observed T_bs (e.g., hours 12:00-15:00 in Fig. 4). Similarly, most of the under-predictions occur in the colder months, when the maximum NM prediction (an active vervet) were closest to the observed T_bs. (e.g., hours 14:00-16:00 in Fig. 4).

3.3.2 Nocturnal hours

NM's maximum, minimum and average (of the maximum and minimum, representing a mix of postures within the group) predicted T_bs during nocturnal hours were compared to observed T_bs (Fig. 3). As expected, during nocturnal hours the minimum T_b prediction was typically lower than the observed T_b, while the maximum T_b prediction typically over estimated T_b compared to observed T_b. The average NM-predicted T_b clustered around observed lower modal T_b. During the first nocturnal hours, NM tended to under-predict T_b (hours 17:00-19:00 in Fig. 5), as the vervets were shifting from active phase T_b to inactive phase T_b. Once the lower modal T_b was reached (hours 21:00 to 06:00 in Fig. 5), the average NM predictions were similar to the observed T_b for spring/fall and summer months. During winter months, the observed T_b was closer to the maximum NM prediction (simulating huddled vervets) for much of the night.

3.4.3 Bracketing Possibilities

As illustrated in the results above, a single model is not appropriate for every given hour. However, the range of potential T_b predictions should encompass the observed T_b for any given hour if the model is accurately calculating T_b. Observed T_bs were within the range of predicted T_bs for >68% of hours and within 0.5°C of the range for >88% of the hours for both the male and female models (Table 3). Removing access to shade (i.e., the minimum T_b prediction is for a vervet resting in the sun) causes a >17% reduction in the percent of diurnal hours for which the predicted range encompasses the observed T_b, resulting entirely from an increased number of overestimated T_b (Table 3). Not allowing huddling (i.e., the maximum predicted T_b is for a curled individual) reduced the percentage of nocturnal hours for which the observed T_b was within the predicted range by ~20% for both sexes. Not allowing curling or huddling resulted in the observed T_b being within 0.5°C of NM's predicted T_b for an uncurled vervet for <20% of the time (Table 4).

Finally, we compared NM's predictions to observed values for several daily T_b metrics (minimum, maximum and mean T_b; 24-hour T_b range) used to assess an animal's thermal performance (e.g., McFarland et al. 2015, Henzi et al. 2017). NM's predicted range was within 0.5°C of observed values for >90% of the days for all of the daily metrics (Table 5). For days when the observed maximum T_b was outside of the predicted range, NM tended to over-predict maximum T_bs. For days when the observed minimum T_b was outside of the predicted range, NM tended to under-predict minimum T_bs. On days when the observed mean T_bs were outside the predicted range, the default models tended to under-predict mean daily T_b, driven by under-predicting overnight T_b in the winter months. Not allowing the animals to seek shade or use different body postures at night reduced model performance (Tables A.4, A.5).

4. DISCUSSION

4.1 Metabolic Chamber and Sensitivity Analyses

To initially assess NMs performance, we placed the vervet model in a simulated metabolic chamber to ensure that NM predicted a reasonable TNZ. We are unaware of any studies reporting a vervet TNZ. There are TNZs reported for several other primate species, and most of these report lower critical temperatures >25°C (Table A.6), higher than the 18-19°C LCT that NM predicted for vervets. However, most of these species are substantially smaller than vervets and/or live in tropical areas with less ambient temperature variability these vervets experience. Species within the Cercopithecidae family in Table A.6 are the most relevant points of comparison in terms of size, ecological, and taxonomic similarity. There is disagreement in the literature even within species, but at least one study for each Cercopithecidae species reports a LCT lower than NM's prediction for vervets. This literature, together with the annual air

temperature range that vervets encounter in the wild (<0°C to >40°C), suggest that NM's predicted TNZ (18/19-28°C) is not unreasonable.

The sensitivity analyses show that most influential biophysical properties were fur depth, hair length:fur depth ratio and body part length:width ratio, and target metabolic rate. All pelage inputs used here were from direct measurements, so we can be confident in their use. The fur thermal conductivities calculated by NM using these fur properties is 0.05-0.07 $Wm^{-1}{}^{\circ}C^{-1}$, depending on body part, consistent with the 0.03 (flattened pelt) - 0.07 (backcombed pelt) $Wm^{-1}{}^{\circ}C^{-1}$ range measured on a vervet pelt (McFarland et al. 2016). The hair length:fur depth ratio is implicated in NM's simulated piloerection and is not relevant for species that lack the ability to piloerect. If this option is allowed, the simulated fur thickness is allowed to increase to 50% of the hair length. Thus, increasing the ratio would allow greater thermal benefits from piloerection. Regarding body sizes and body part dimensions, the sensitivity analyses illustrate how the model predicts that larger vervets or more compact animals will be more cold-tolerant. It is interesting that the uncurled male and female models are predicted to have a similar TNZ despite males being 45% larger than females. However, the females were more compact (smaller body part length-to-width ratios) and had relatively thicker fur, both of which appear to offset the thermal effect of smaller body size.

Our resting metabolic rate is justified since NM's default resting metabolic rate regression provides a good approximation of resting metabolic rates measured in haplorhine primates of similar size to vervets (3-6 kg), and interspecies variation is less than 10% from that regression line (Fig. A.2, Table A.2). However, the choice of monthly activity multipliers that dictate the target metabolic rate for the "active" simulations may affect our results. To analyze the effect of this parameter choice, we performed a sensitivity analysis comparing the results

using the activity multipliers as stated in the methods above to two alternate scenarios: 1) using a constant multiplier of 2.75x BMR for all months of the year, and, 2) muting the seasonal variation in activity multipliers to range from 2.5x BMR in the summer and 3.6x BMR in the winter (i.e., cutting the variation in half, as measured from deviations from the constant 2.75x BMR). The muted response reduced the number of diurnal hours where observed T_b was within the range of predicted T_bs by <5% and reduced the number of diurnal hours where the predicted range was within 0.5°C of the observed T_b by <2% (Table A.8). Assuming a constant activity multiplier throughout the year reduced the number of diurnal hours where observed T_b was within the range of predicted T_b s by 8-10% and reduced the number of diurnal hours where the predicted range was within 0.5°C of the observed T_b by <5% (Table A.8). Changing the activity multiplier assumptions has a similar effect on predicted daily maximum T_b, predicted daily mean T_b and 24-hour amplitude predictions (Table A.9). Given the seasonal variation in vervet activity patterns (McFarland et al. 2014) a constant activity multiplier is unrealistic, but these results nevertheless illustrate the effect of this parameter choice. Importantly, if we were to halve the seasonal variation in activity multipliers in our models, our primary conclusions would have remained the same.

The maximum winter activity multiplier results in a 24-hour activity level of 2.46x RMR, which would be on the higher end of daily activity levels reported from limited information on primates (Simmen et al. 2015). However, reducing winter activity multipliers results in NM under-predicting more diurnal T_bs in the winter. An alternative explanation is that there could be undetected seasonal changes in fur properties (e.g., thicker and/or denser fur in the winter vs. summer), which would allow NM to predict higher winter T_bs using a lower activity multiplier.

However, this appears unlikely, given the authors have not observed a visible change in vervet pelage between seasons.

Our sensitivity analyses identified the biophysical properties that most strongly influence NM's T_b and metabolic rate predictions. Gathering information on these parameters should therefore be a priority for other researchers interested in using biophysical models to examine the thermal performance of other species. To validate NM's ability to predict body temperature in the current study, it was essential that we had detailed measures of, not only vervet morphology, but also accurate measures of core body temperature. However, since NM's animal submodel is generic, and can be used for any species, our study's validation should give confidence to those interested in using NM to make predictions, in the absence of such a detailed data set. Indeed, NM has been used to effectively examine the thermal performance of a range of species, including extinct species in historical climate scenarios (Porter et al. 2006, Wang et al. 2018, Lovelace et al. 2020).

If study-specific information for particular model inputs were unavailable, the existing literature on a given, or closely-related, species, can often be used to provide reasonable estimates of resting metabolic rate, T_b, the ability to pant or sweat, posture, and microclimate options (e.g., shade-use). Similarly, pelage properties can often be found in the literature (or reasonably estimated from similar species with values in the literature). Museum or other taxidermic specimens are also good sources of obtaining necessary pelage property inputs. Body part dimensions, if unavailable in the literature, can be estimated based on animal photographs, that can be scaled up based on the known size of the animal (see e.g., Mathewson & Porter 2013).

4.2 Body Temperature Predictions

In this first test of NM's ability to predict T_b in wild animals, predicted maximum and minimum T_bs bracketed the observed T_b for the majority of hours (Tables 3,4). Importantly, although T_bs in NM were allowed to fluctuate above and below the observed upper and lower modal T_bs observed in the wild vervets, the "average" predicted T_b clustered around the upper modal T_b during the day and the lower modal T_b during the night (Fig. 3). This finding indicates that NM was able to capture a vervet's typical response to fluctuating environmental conditions and provides confidence that other outputs that are dependent on T_b, like metabolic rate and evaporative water loss, are also likely to be reliable. More fundamentally, it supports the idea that temporal T_b variability is an emergent property of animals trying to maintain a certain metabolic rate rather than animals modifying their metabolic rate to maintain a given T_b.

Deviations >0.5°C between observed and the "average" predicted T_b were sometimes observed. However, they follow logical patterns based on the time of day and time of year. For diurnal hours, most of the over-predictions occurred in the warmer months when vervets have been observed to reduce activity (McFarland et al. 2014). Thus, the "average" prediction would be expected to over-predict T_b because the "resting" prediction would be more appropriate for these hours. Similarly, most of the under-predictions occur in the colder months. On the colder days vervets have been shown to increase activity and foraging time (McFarland et al. 2014), and it is unlikely there will be much shade-seeking in the winter. Thus, the "average" prediction would be expected to under-predict T_b because the "active" prediction would be more appropriate for these hours. Furthermore, the T_b cycling could be an entrained daily rhythm regardless of given day's air temperature (Levesque et al. 2016), even at the potential cost of additional heat loss on the coldest days of the year. NM does not have a built-in T_b cycling. All

predicted deviations from the specified starting T_b (38°C) are due to responses to environmental conditions and the required metabolic rates to either minimize metabolic heat production (T_b reductions in cold conditions) or to maintain minimum metabolic heat production (T_b increases in hot conditions).

More activity than usual on a given day could also cause NM to under-predict daytime T_b because our modeling assumed the same activity level for all days within a month for its "active" prediction. NM's T_b predictions also do not include the heat increment of feeding, potentially leading to under-predictions in post-feeding hours. Occasional swimming and drinking of cool water have also been observed in this group (McFarland et al. 2020), which could account for some T_b over-predictions in the warmer months. Finally, we do not simulate the effect of rainfall cooling the microenvironment or wetting the vervets' pelage, which could result in some T_b over-predictions.

Regarding nocturnal T_b, for the first hours after sunset, NM under-predicts T_b (hours 17:00 and 18:00 in Fig. 5). This is likely due to NM assuming an immediate metabolic rate reduction from active to resting to occur at sundown. In reality, there may be some crepuscular activity of vervets in the trees as they settle down for the night, and vervets may have a more gradual metabolic rate reduction from active to resting. While the most common average nocturnal prediction was close to the observed T_b (see Fig. A.9) there are hours when the "average" prediction over- or under-predicts the observed T_b by >2°C. These discrepancies could result from the majority of individuals in the group choosing a more or less heat-conserving posture on certain nights, causing the "average" prediction to over-predict T_bs on hot nights (e.g., if most individuals choose to stretch out) or to under-predict T_bs on cold nights (e.g., if most individuals choose to huddle).

Some over-predictions could also be due to the observed T_b cycling potentially being an entrained rhythm that occurs daily, even if the nighttime T_b reduction is not necessary to minimize heat loss on a particular day as discussed above with diurnal T_bs. Some under-predictions could be due to vervets increasing metabolic rates to defend their lower modal T_b. For example, in some conditions it could be worth the extra metabolic expenditure to maintain a preferred T_b, provided that sufficient food resources are available to supply this additional energetic demand. In contrast, NM's thermoregulatory decision-making always chooses to minimize metabolic heat production and will reduce T_b in such situations. Specific to females, female reproductive state or having a dependent infant could explain some discrepancies. Females with a clinging infant will have less heat loss to the environment, and gestational hypothermia was observed in pregnant females.

4.3 Study implications

Vervets, like all endotherms, must balance maintaining their body temperature with the thermoregulatory costs incurred to do so, all the while engaging in activities necessary for survival and reproduction. A biophysical model that can accurately model an animal's fundamental energetic interactions with its environment allows quantification of thermoregulatory costs (e.g., increased metabolic heat production or evaporative water loss requirements, reduced activity time) and exploration of other questions about the fitness implications of a species' morphology, physiology and behavior in relation to its environment. For example, our results here provide support for the ideas of Lubbe et al. (2014), McFarland et al. (2015, 2016), and Henzi et al. (2017), that the observed heterothermy and huddling help improve fitness by reducing energetic costs during the cold winters experienced by this vervet group (as evidenced by NM utilizing an overnight T_b lower than the starting point T_b to minimize

metabolic heat production needed to maintain resting metabolic rate and huddled model T_b predictions providing the best match to observed T_b in the winter). Such models can also provide insight into the importance of certain habitat characteristics, such as shade availability, to reduce heat-related costs or access to water to facilitate the use of evaporative cooling to thermoregulate (McFarland et al. 2020).

As illustrated by our sensitivity analyses showing how body size and limb dimension affect thermal tolerance, such a model could also be used to investigate whether spatial variation in morphology across a species' range could confer energetic advantages (e.g., Bergmann's and Allen's rule). Biophysical models could be also be used to explore how disparate morphology, physiology and/or behavior between sympatric species could play a role in niche partitioning. Since the microclimate model can be parameterized with any set of environmental conditions, similar analyses could be extended into the past to explore past distributions and/or morphological changes from present may have been necessary for the species to survive in past environmental conditions (e.g., Mathewson et al. 2017, Lovelace et al. 2020). Such investigations could provide insight into the evolutionary history of a species.

Looking forward in time, having an accurate biophysical model can provide insight into species responses to changing environments, either from climate change or land cover changes. In some places natural forest is being replaced by monocrop tree plantations, presumably resulting in hotter and drier environments that may impose thermoregulatory stress on some animals and affect the likelihood that such environments could serve as suitable habitat (Spehar and Rayadin 2017). In the context of exploring species' response to climate change, biophysical models enable a mechanistic approach to species distribution modeling. Such models allow researchers to investigate how direct effects of the climate on animals (e.g., enforced resting to

avoid heat stress) constrain distributions. Explicitly modeling the mechanism by which climate is thought to limit distributions may provide more accurate predictions of future distributions and is an important research area in need of development, particularly for endotherms (e.g., Buckley et al. 2012, Evans et al. 2015).

ACKNOWLEGEMENTS

We are grateful to Mark, Sarah and Isabelle Tompkins for permission to work at the Samara Private Game Reserve. This research was funded by Faculty research grants from the University of the Witwatersrand, a Claude Leon Fellowship awarded to RM, NSERC Canada Discovery grants to LB and SPH, the Canada Research Chair program to LB, South African National Research Foundation grants to AF, RH, and SPH, and a Carnegie Large Research grant to AF. Finally, we thank seven anonymous reviewers and the editorial staff for valuable critiques that have improved this manuscript.

REFERENCES

Briscoe NJ, Kearney MR, Taylor C, Brendan WA (2016) Unpacking the mechanisms captured by a correlative SDM to improve predictions of a climate refugia. Global Change Biology 22: 2425-2439.

Buckley LB, Kingsolver JG (2012) Functional and phylogenetic approaches to forecasting species' responses to climate change. Annual Review of Ecology, Evolution, and Systematics 43: 205-226.

Buckley LB, Urban MC, Angilletta MJ, Crozier LG, Rissler LJ, Sears MW (2010) Can mechanism inform species' distributional models. Ecology Letters 13: 1041-1054.

Buckley LB, Hurlbert AH, Jetz W (2012) Broad-scale ecological implications of ectothermy and endothermy in changing environments. Global Ecology and Biogeography 21: 873-885.

Cantaloup C, Borgeaud C, Wubs M, van de Wall E. 2019. The effect of social and ecological factors on the time budget of wild vervet monkeys. Ethology 125: 902-913.

Cho BT, editor (1969) Advanced Heat Transfer. Urbana, IL: U Illinois Press. 459 pp.

Conley KE, Porter WP (1986) Heat loss from deer mice (Peromyscus): evaluation of seasonal limits to thermoregulation. Journal of Experimental Biology 126: 249-269.

Dunbar RIM, Korstjens AH, Lehmann J (2009) Time as an ecological constraint. Biological Reviews 84: 413-429.

Dormann, CF, Schymanski SJ, Cabral J, et al. (2012) Correlation and process in species distribution models: bridging a dichotomy. Journal of Biogeography 39: 2119-2131.

Elith J, Leathwick JR. (2009) Species distribution models: ecological explanation and prediction across time and space. Annual Review of Ecology, Evolution, and Systematics 40: 677-697.

Estrada A, Garber PA, Rylands AB et al. (2017) Impending extinction crisis of the world's primates: why primates matter. Science Advances 3: e1600946

Evans TG, Diamond SE, Kelly MW (2015) Mechanistic species distribution modelling as a link between physiology and conservation. Conservation Physiology 3: doi:10.1093/conphys/cov056

Fuentes M, Porter WP (2013) A new approach to model soil temperature: using microclimate models to predict the impacts of climate change on sea turtles. Ecological Modeling 251: 150–157.

Fuller A, Dawson T, Helmuth B, Hetem RS, Mitchell D, Maloney SK (2010) Physiological mechanisms in coping with climate change. Physiological and Biochemical Zoology 83: 713-720.

Fuller A, Mitchell D, Maloney SK, Hetem RS (2016) Towards a mechanistic understanding of the responses of large terrestrial mammals to heat and aridity associated with climate change. Climate Change Responses 3: 10.

Gordon MS, Bartholomew GA, Grinnell AD, Jorgensen CB, White FN (1972) Animal Physiology: Principles & Adaptations (2nd ed). Macmillan Publ. Co., London. 592 pp.

Henzi SP, Hetem R, Fuller A, Maloney SK, Young C, Mitchell D, Barrett L, McFarland R (2017) Consequences of sex-specific sociability for thermoregulation in male vervet monkeys during winter. Journal of Zoology 302: 193-200.

Hetem RS, Maloney SK, Fuller A, Mitchell D (2016) Heterothermy in large mammals: inevitable or implemented. Biological Reviews 91: 187-205.

Hijmans RJ, Graham CH (2006) The ability of climate envelope models to predict the effect of climate change on species distributions. Global Change Biology 12: 2272-2281.

Huey RB, Kearney MR, Krockenberger A, Holtum JAM, Jess M, Williams SE (2012) Predicting organismal vulnerability to climate warming: roles of behaviour, physiology and adaptation. Philosophical Transactions of The Royal Society B. 36: 1665-1679.

Kearney M, Porter WP (2009) Mechanistic niche modelling: combining physiological and spatial data to predict species' ranges. Ecology Letters 12: 334-350.

Korstjens AH, Lehmann J, Dunbar RIM (2010) Resting time as an ecological constraint on primate biogeography. Animal Behaviour 79: 361-374.

Lacombe A (2002) Effects of temperature on metabolism, ventilation, and oxygen extraction in the Southern Brown Bandicoot *Isoodon obesulus* (Marsupialia: Peramelidae). Physiological and Biochemical Zoology 4: 405-411.

Lehmann J, Korstjens AH, Dunbar RIM (2010) Apes in a changing world—the effects of global warming on the behavior and distribution of African apes.

Levesque DL, Nowack J, Stawski C (2016) Modelling mammalian energetics: the heterothermy problem. Climate Change Responses 3: 7.

Long RA, Bowyer RT, Porter WP, Mathewson PD, Monteith KL, Kie JG (2014) Behaviour and nutritional condition buffer a large-bodied endotherm against direct and indirect effects of climate. Ecological Monographs 84: 513-532.

Lovelace DM, Hartman SA, Mathewson PD, Linzmeier BJ, Porter WP. (2020) Modeling Dragons: Using linked mechanistic physiological and microclimate models to explore environmental, physiological, and morphological constraints on the early evolution of dinosaurs. PLOS ONE 15:e0223872

Lubbe A, Hetem RS, McFarland R, et al. (2014) Thermoregulatory plasticity in free-ranging vervet monkeys, *Chlorocebus pygerythrus*. Journal of Comparative Physiology B., Biochemical, systemic, and environmental physiology 184:799–809.

Mason THE, Brivio F, Stephens PA, Apollonio M, Grignolio S (2017) The behavioral trade-off between thermoregulation and foraging in a heat-sensitive species. Behavioral Ecology 28: 908-918.

Mathewson PD (2018) Biophysical models as tools to improve understanding of endotherm responses to environmental change. PhD dissertation, Department of Zoology, University of Wisconsin, Madison, Wisconsin, USA.

Mathewson PD, Porter, WP (2013) Simulating polar bear energetics during a seasonal fast using a mechanistic model. PLoS One 8: e72863.

Mitchell D, Fuller A, Maloney SK (2009) Homeothermy and primate bipedalism: is water shortage or solar radiation the main threat to baboon (*Papio hamadryas*) homeothermy? Journal of Human Evolution 56: 439-446.

Mitchell D, Snelling EP, Hetem RS, Maloney SK, Strauss WM, Fuller A (2018) Revisiting concepts of thermal physiology: predicting responses of mammals to climate change. Journal of Animal Ecology 87: 956-973.

McFarland R, Barrett L, Boner R, Freeman NJ, Henzi SP (2014) Behavioral flexibility of vervet monkeys in response to climatic and social variability. American Journal of Physical Anthropology 154:357–364.

McFarland R, Fuller A, Hetem RS, Mitchell D, Maloney SK, Henzi SP, Barrett L (2015) Social integration confers thermal benefits in a gregarious primate. Journal of Animal Ecology 84:871–878.

McFarland R, Henzi S, Barrett L (2019) The social and thermal competence of wild vervet monkeys. In Turner T (Ed.): Savanna monkeys: the genus Chlorocebus (pp. 119-207). Cambridge University Press.

McFarland R, Barrett L, Fuller A, Hetem RS, Maloney SK, Mitchell D & Henzi SP (2020) Keeping cool in the heat: Behavioral thermoregulation and body temperature patterns in wild vervet monkeys. American Journal of Physical Anthropology 171: 407-418.

McFarland R, Henzi SP, Barrett L, Wanigaratne A, Coetzee E, Fuller A, Hetem RS, Mitchell D, Maloney SK (2016) Thermal consequences of increased pelt loft infer an additional utilitarian function for grooming. American Journal of Primatology 78: 456-461.

McFarland R, Barrett L, Fuller A, Hetem RS, Maloney SK, Mitchell D & Henzi SP. 2019. Keeping cool in the heat: Behavioral thermoregulation and body temperature patterns in wild vervet monkeys. American Journal of Physical Anthropology 171: 407-418.

Moyer-Horner L, Mathewson PD, Jones G, Kearney MR, Porter WP (2015) Modeling behavioral thermoregulation in a climate change sentinel. Ecology and Evolution 5**:** 5810-5822.

Müller EF, Kamau JMZ, Maloiy GMO (1983) A comparative study of basal metabolism and thermoregulation in a folivorous (*Colobus guereza*) and an omnivorous *(Cercopithecus mitis*) primate species. Comparative Biochemistry and Physiology. A, Comparative physiology 74: 319-322.

Natori Y, Porter WP (2007) Model of Japanese Serow (*Capricornis crispus*) energetics predicts distribution on Honshu, Japan. Ecological Applications 17: 1441-1459.

New M, Lister D, Hulme M, Makin I (2002) A high-resolution data set of surface climate over global land areas. Climate Research 21: 1-25.

Pacifici M, Foden WB, Visconti P, et al. (2015) Assessing species vulnerability to climate change. Nature Climate Change 5: 215-224.

Pasternak G, Brown LR, Kienzle S, Fuller A, Barrett L, Henzi SP (2013) Population ecology of vervet monkeys in a high latitude, semi-arid riparian woodland. Koedoe 55:1–9.

Porter WP (2016) Heat Balances in Ecological Contexts. A Biogeoscience Approach to Ecosystems. E. A. Johnson and Y. E. Martin. Cambridge, Cambridge University Press**:** 49-87

Porter WP, Gates DM (1969) Thermodynamic equilibria of animals with environment. Ecological Monographs 39: 227-244.

Porter WP, Mitchell JW (2006) Method and system for calculating the spatial-temporal effects of climate and other environmental conditions on animals. http://www.warf.org/technologies.jsp?ipnumber=P01251US

Porter WP, Vakharia N, Klousie WD, Duffy D (2006) Po'ouli landscape bioinformatics models predict energetics, behavior, diets, and distribution on Maui. Integrative and Comparative Biology 46: 1143-1158.

R Core Team (2017) R: A language and environment for statistical computing. R Foundation for Statistical Computing, Vienna, Austria. URL https://www.R-project.org/.

Seebacher F, Little AG (2017) Plasticity of performance curves can buffer reaction rates from body temperature variation in active endotherms. Frontiers in Physiology 8: 575 doi: 10.3389/fphys.2017.00575

Simmen B, Darlu P, Hladik CM, Pasquet P. 2015. Scaling of free-ranging primate energetics with body mass predicts low energy expenditure in humans. Physiology & Behavior 138: 193-199.

Smith NP, Barclay CJ, Loiselle DS (2005) The efficiency of muscle contraction. Progress in Biophysics & Molecular Biology 88: 1-58.

Speakman JR, Krol E (2010) Maximal heat dissipation capacity and hyperthermia risk: neglected key factors in the ecology of endotherms. Journal of Animal Ecology 79: 726-746.

Spehar SN, Rayadin Y (2017) Habitat use of Bornean orangutans (*Pongo pygmaeus morio*) in an industrial forestry plantation in East Kalimantan, Indonesia. International Journal of Primatology 38: 358-384.

Urban MC, Bocedi G, Hendry AP, et al. (2016) Improving the forecast for biodiversity under climate change. Science 353: 6304

Wang Y, Porter W, Mathewson PD, Miller PA, Graham R, Williams JW. 2018. Mechanistic modeling of environmental drivers of woolly mammoth carrying capacity declines on St. Paul Island. Ecology 99: 2721-2730.

Zhang Y, Mathewson PD, Zhang Q, Porter WP, Ran J (2018) An ecophysiological perspective on likely giant panda habitat responses to climate change. Global Change Biology 24: 1804-1816.

Table 1. Relevant biophysical properties used to parameterize Niche Mapper's animal model for vervet monkeys. Data are sourced from the current study (mean±S.D.) unless marked with superscript. Variation is shown to demonstrate variability between individuals to provide additional context for the sensitivity analyses; mean values used in the modeling. These inputs were used in the thermoneutral zone and wild vervet T_b validation modeling and were the starting points for the sensitivity analyses.

Parameter	*Female*	*Male*
Body mass (kg)[a]	3.4-3.6	4.7-5.0
Head		
Vertical/horizontal diameter (mm)	88±3/87±7	95±1/96±14
Length (mm)	122±3	133±10
Fur depth (mm)	19±2	21±4
Hair length: fur depth ratio	2.1±0.1	2.1±0.1
Torso		
Vertical/horizontal diameter (mm)	143±10/124±0	173±11/148±15
Length (mm)	350±10	390±7
Dorsal/ventral fur depth (mm)	15±0/18±3	15±5/21±6
Dorsal/ventral hair length: fur depth ratio	2.1±0.6/3.2±0.4	2.1±0.6/3.2±0.4
Arms		
Vertical/horizontal diameter (mm)	42±3/39±1	54±4/43±4
Length (mm)	180±0	215±11
Fur depth (mm)	11±1	11±4
Hair length: fur depth ratio	2.7±0.5	2.7±0.5
Legs		
Vertical diameter (mm)	72±15	78±15
Horizontal diameter (mm)	49±10	55±6
Length (mm)	220±20	265±27
Fur depth (mm)	13±3	13±6
Hair length: fur depth ratio	3.6±0.1	3.6±0.1
Tail		
Vertical/horizontal diameter (mm)	24±10/24±1	25±0/28±2
Length (mm)	505±55	575±102
Fur depth (mm)	7±4/26	7±4/26
Hair length: fur depth ratio	4.0±0	4.0±0
Hair solar reflectivity (%)[b]	20±1.3	
Hair diameter (μm)	30	
Hair density (no. cm^{-2})	1600	
Resting metabolic rate (W)[c]	3.39 x mass $(kg)^{0.75}$	
Core body temperatures (ºC)[d]	Starting 38; Min: 36; Max: 41	
Flesh thermal conductivity ($Wm^{-1}{}^{\circ}C^{-1}$)[e]	Starting: 1.0; Min: 0.4; Max: 2.8	
O_2 extraction efficiency (%)[f]	20	
Activity energy included in heat balance (%)[g]	80	

[a] Average body mass of the subset of study animals implanted varied by field season
[b] Vervet monkey pelage heat-transfer characteristics (McFarland et al. 2016)
[c] Regression for placental mammals (Gordon et al. 1972) used as a default in Niche Mapper. Provides a good fit with data from published studies of primate metabolic rates (Fig. A.2, Table A.2).

[d] T_b was held constant at 38°C for the thermoneutral zone modeling and all sensitivity analyses except the T_b variability analysis

[d] Thermophysical property data on biological media, including a cold living hand (0.34 $Wm^{-1}C^{-1}$), very warm living skin (2.8 $Wm^{-1}{}^{\circ}C^{-1}$) (Cho 1969).

[e] Mammal O_2 extraction efficiency is typically 20% (Lacombe 2002).

[f] Based on measurements of mammalian muscle efficiency being ~20% as measured in rats and mice (Smith et al. 2005).

Table 2. Summary of vervet model sensitivity analysis results showing the changes in whole body thermal conductivity (WBTC), upper critical air temperature (UCT) and lower critical air temperature (LCT) in response to 10% and 25% changes in key biophysical parameters. Values shown are for the female model; similar trends were observed for the male model. NC= No change.

		10% Increase	10% Decrease	25% Increase	25% Decrease
Fur depth	WBTC	-3%	6%	-13%	+22%
	UCT	-1°	+1°	-1°	+2°
	LCT	NC	+2°	-2°	+3°
Hair density	WBTC	-3%	3%	-6%	+9%
	UCT	NC	+1°	NC	+1°
	LCT	-1°	+1°	-2°	+2°
Hair diameter	WBTC	-3%	3%	-6%	+9%
	UCT	NC	+1°	NC	+1°
	LCT	-1°	+1°	-1°	+2°
Hair length: fur depth ratio	WBTC	-9%	+9%	-20%	+34%
	UCT	NC	+1°	NC	+1°
	LCT	-2°	+2°	-6°	+5°
Total body mass	WBTC	2%	11%	-8%	+21%
	UCT	NC	+1°	NC	+1°
	LCT	NC	+1°	-1°	+2°
Body part lengths	WBTC	+6%	-9%	+16%	-17%
	UCT	+1°	-1°	+2°	-2°
	LCT	+1°	-1°	+3°	-5°
Resting Metabolic Rate	WBTC	NC	NC	NC	NC
	UCT	-1°	+1°	-3°	+3°
	LCT	-2°	+2°	-6°	+6°

Table 3. Percentage of diurnal hours in the 2012-2016 field seasons (n=14,037) that the mean observed vervet body temperature (T_b) was within NM's predicted T_b range (encompassing an active individual in full sun and an inactive individual with and without access to shade). Also shown are the percentage of hours that the observed T_b was within 0.5° or 1° C of the predicted range. In parentheses are the number of hours for which the predicted range was over/under the observed T_b. Removing shade access increased the number of hours that NM overpredicted T_b.

		Shade Available	**No Shade Available**
Females	Within Range	72.6% (1669/2018)	54.4% (4108/2018)
	Within 0.5°C	93.7% (378/472)	84.9% (1563/472)
	Within 1.0°C	99.4% (51/25)	96.6% (437/25)
Males	Within Range	67.6% (1940/2418)	48.8% (4466/2418)
	Within 0.5°C	91.3% (621/542)	82.3% (1843/542)
	Within 1.0°C	98.8% (131/31)	95.4% (587/31)

Table 4. Percentage of nocturnal hours in the 2012-2016 field seasons (n=13443) that the mean observed vervet body temperature (T_b) was within NM's predicted T_b range (encompassing different body postures). Also shown are the percentage of hours that the observed T_b was within 0.5° or 1°C of the predicted range. In parentheses are the number of hours for which the range predicted by NM was over/under the observed T_b. "Stretched only" refers to only modeling a lone, uncurled individual (no range); "Stretched + curled" refers the range of T_bs predicted between an uncurled individual and a curled (arms and legs tucked into torso) individual; "Stretched + curled + huddled" refers to the range of T_bs predicted between an uncurled individual and an individual huddled between two others.

		Stretched + curled + huddled	**Stretched + curled**	**Stretched only**
Females	Within Range	70.4% (750/3230)	45.7% (750/6553)	NA
	Within 0.5°C	87.8% (215/1424)	66.5% (215/4292)	14.9% (215/11228)
	Within 1.0°C	98% (43/228)	89.8% (43/1330)	53% (43/6277)
Males	Within Range	73.4% (857/2715)	53.1% (857/5450)	NA
	Within 0.5°C	90.4% (256/1039)	74.9% (256/3114)	18.4% (256/10711)
	Within 1.0°C	98.1% (45/217)	92.3% (45/989)	60.2% (45/5308)

Table 5. Percentage of days in the 2012-2016 field seasons (n=1145) that the mean observed minimum, maximum, average, and 24 hour-amplitude vervet body temperature (T_b) was within the boundaries of NM's predicted T_b between the coldest model (lone monkey stretched out at night; resting in shade during the day) and the warmest model (huddled at night; active in sun during the day). Also shown are the percentage of days that the observed metric was within 0.5° or 1°C of the predicted range. In parentheses are the number of days for which the range predicted by NM was over/under the mean observed metric.

			Female	**Male**
Minimum	T_b	Within Range	82% (17/189)	87.3% (48/97)
		Within 0.5°C	91% (5/98)	97.4% (5/25)
		Within 1.0°C	99.1% (1/9)	99.7% (0/3)
Maximum	T_b	Within Range	78.4% (139/108)	72.8% (146/165)
		Within 0.5°C	96.2% (33/10)	94.9% (42/16)
		Within 1.0°C	99% (11/0)	99.1% (10/0)
Mean T_b		Within Range	90.4% (29/81)	91.3% (39/61)
		Within 0.5°C	99.8% (0/2)	99.6% (1/4)
		Within 1.0°C	100% (0/0)	100% (0/0)
24-hour T_b	Amplitude	Within Range	97.3% (15/16)	93.9% (2/68)
		Within 0.5°C	99.9% (0/1)	98.2% (0/21)
		Within 1.0°	99.9% (0/1)	99.7% (0/3)

Figure 1. Schematic showing the relationship between Niche Mapper's microclimate and animal submodels as well as the inputs required by the respective submodel for Niche Mapper's heat balance calculations.

Figure 2. Example plots of NM's hourly predicted body temperatures (T_b) and hourly observed female T_b for a winter month (a; August 2014) and a summer month (b; December 2014). The maximum predicted T_b is for a monkey active in sun for diurnal hours and a huddled monkey for nocturnal hours. The minimum predicted T_b is for a monkey inactive in full shade for diurnal hours and for an uncurled monkey for nocturnal hours. The shaded gray area shows the range of observed T_b for a given hour. Air temperatures are also shown for reference.

Figure 3. Plots of predicted vs. observed female body temperature (T_b). For diurnal hours, the minimum NM T_b is for a vervet inactive in the shade; the maximum NM T_b is for a vervet active in the sun. An average of the maximum and minimum T_b predictions, representing a mix of activity and inactivity, is also shown. For nocturnal hours, predictions are shown for different nighttime postures uncurled (minimum T_b prediction), curled, and huddled (maximum T_b prediction). The average prediction is the average of the maximum and minimum T_b nocturnal predictions. The darker the color of the hexagon, the greater the number of hourly T_b comparisons in that plot location. The dashed lines indicate the observed modal T_bs (lower overnight T_b and higher daytime T_b) of the wild vervets; the solid line indicates a 1:1 relationship between observed and predicted T_b. Similar trends were observed for the male model.

Figure 4. The difference (±S.D.) between observed and predicted female body temperatures (T_b) for diurnal hours between 2012 and 2016. Data are broken down by hour (04:00-18:00) and season (summer = December-February; winter = June-August; spring=March-May; fall=September-November). The minimum NM T_b is for a vervet inactive in the shade; the maximum NM T_b is for a vervet active in the sun. The average prediction is the average of the maximum and minimum T_b predictions, representing a mix of activity and inactivity. For 04:00 and 18:00 hours, daylight is only present for a summer month. Similar trends were observed for the male model (Fig. A.10).

Figure 5. The difference (± S.D.) between observed and predicted body temperatures (T_b) for nocturnal hours between 2012 and 2016. The data are broken down by hour (17:00-06:00) and season (summer = December-February; winter = June-August; spring/fall=March-May; September-November). The minimum NM T_b is for a lone uncurled vervet; the maximum NM T_b is for a huddled vervet. The average prediction is the average of the maximum and minimum T_b predictions, representing a mix of postures. For 06:00, sunlight was absent only for a winter month. Similar trends were observed for the male model (Fig. A.11).

Figure 1.

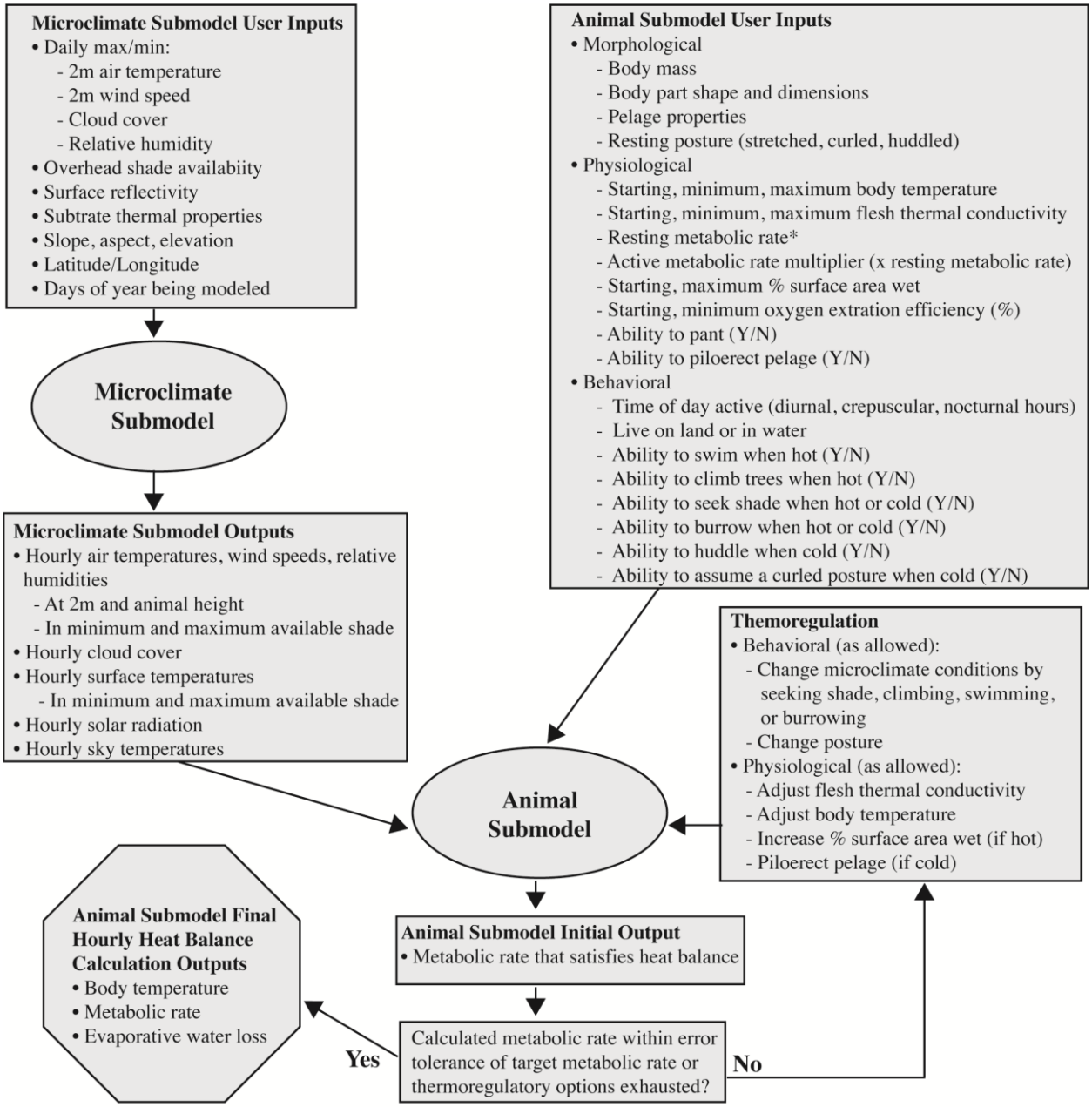

* Users can optionally enter a resting metabolic rate. If no data are available, the model's default resting metabolic rate is a generic mammalian regression relationship between animal mass and resting metabolic rate.

Figure 2.

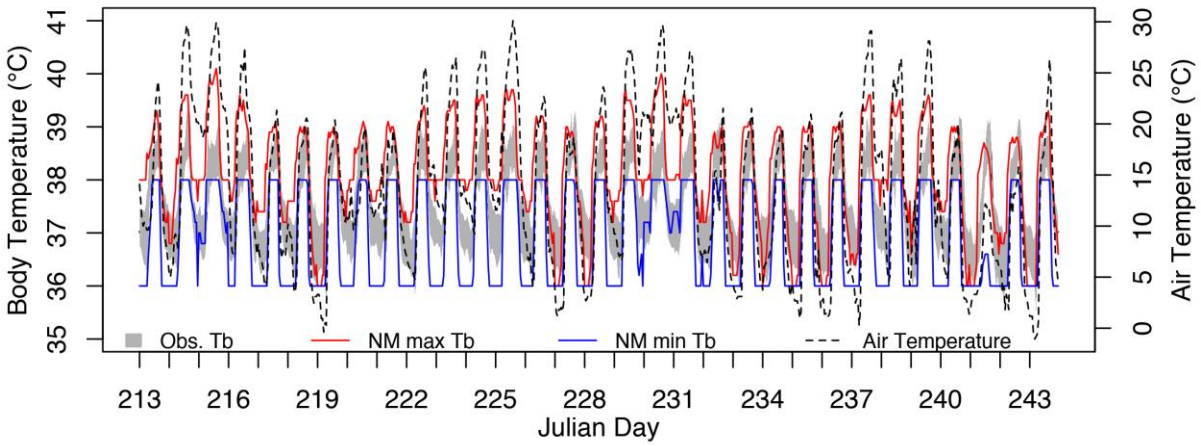
Body Temperature (°C)
Air Temperature (°C)
Obs. Tb
NM max Tb
NM min Tb
Air Temperature
Julian Day

(a)

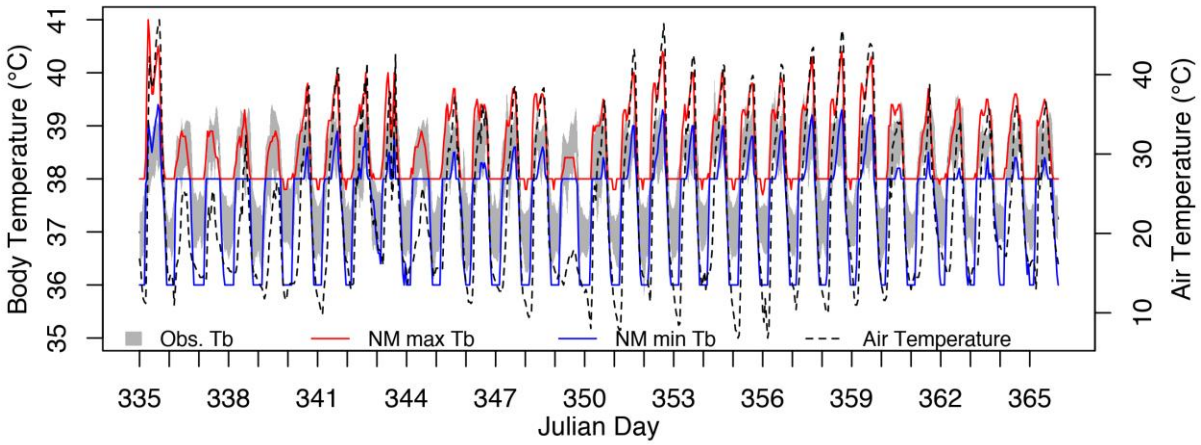
Body Temperature (°C)
Air Temperature (°C)
Obs. Tb
NM max Tb
NM min Tb
Air Temperature
Julian Day

(b)

Figure 3.

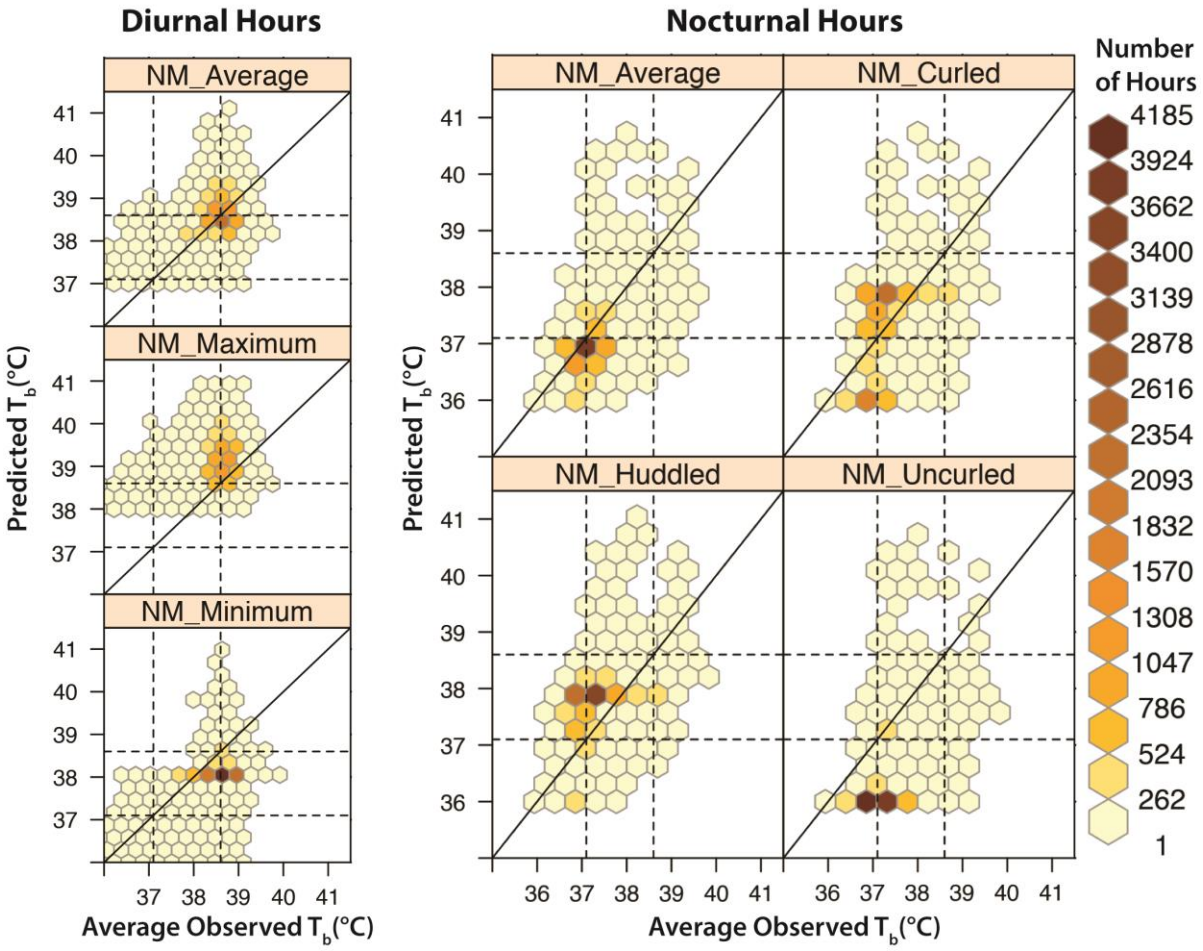
Diurnal Hours
Nocturnal Hours
NM_Average
NM_Maximum
NM_Minimum
NM_Average
NM_Curled
NM_Huddled
NM_Uncurled
Predicted T_b(°C)
Average Observed T_b(°C)
Number of Hours
4185
3924
3662
3400
3139
2878
2616
2354
2093
1832
1570
1308
1047
786
524
262
1

Figure 4.

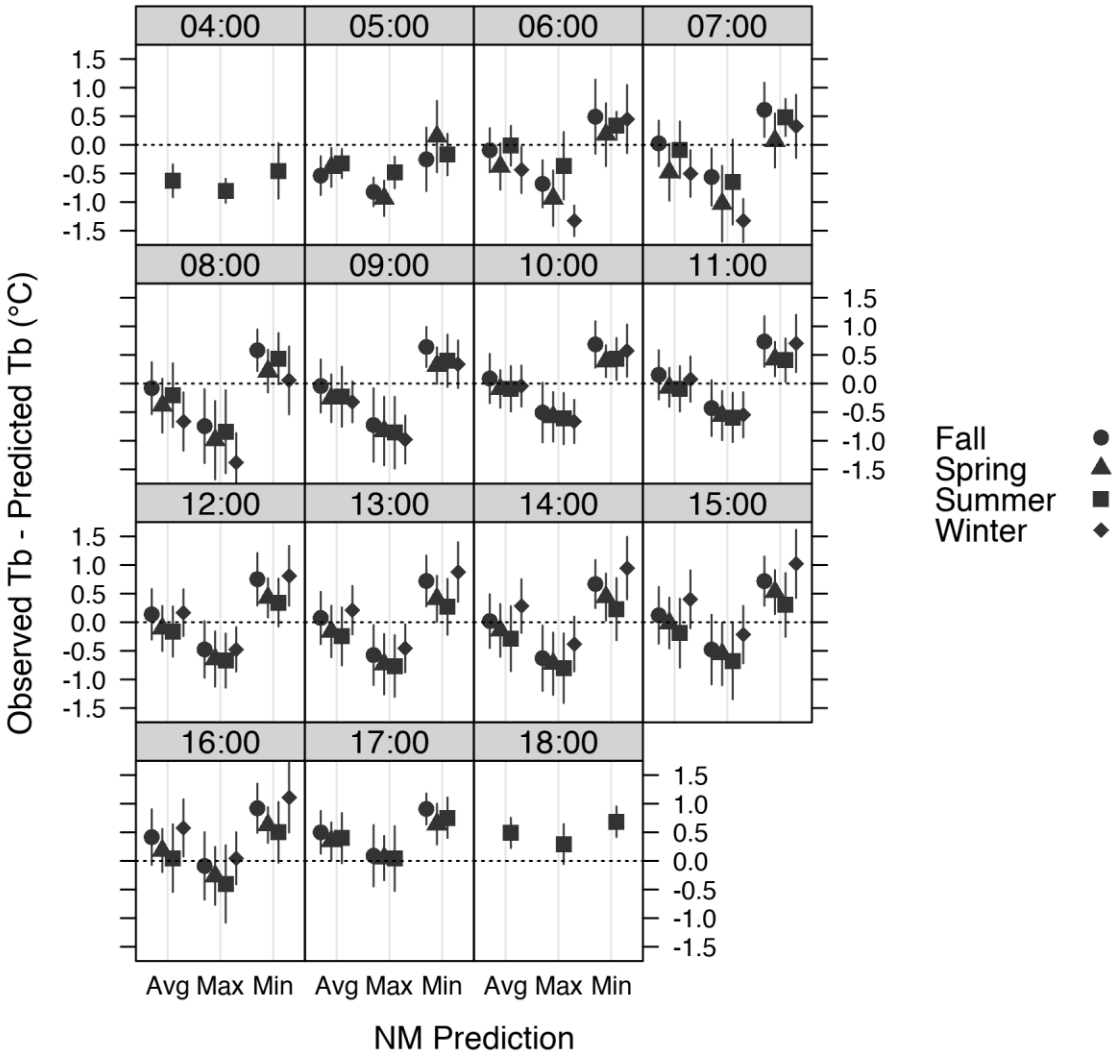
04:00
05:00
06:00
07:00
08:00
09:00
10:00
11:00
12:00
13:00
14:00
15:00
16:00
17:00
18:00
1.5
1.0
0.5
0.0
-0.5
-1.0
-1.5
Observed Tb - Predicted Tb (°C)
Avg Max Min
NM Prediction
Fall
Spring
Summer
Winter

Figure 5.

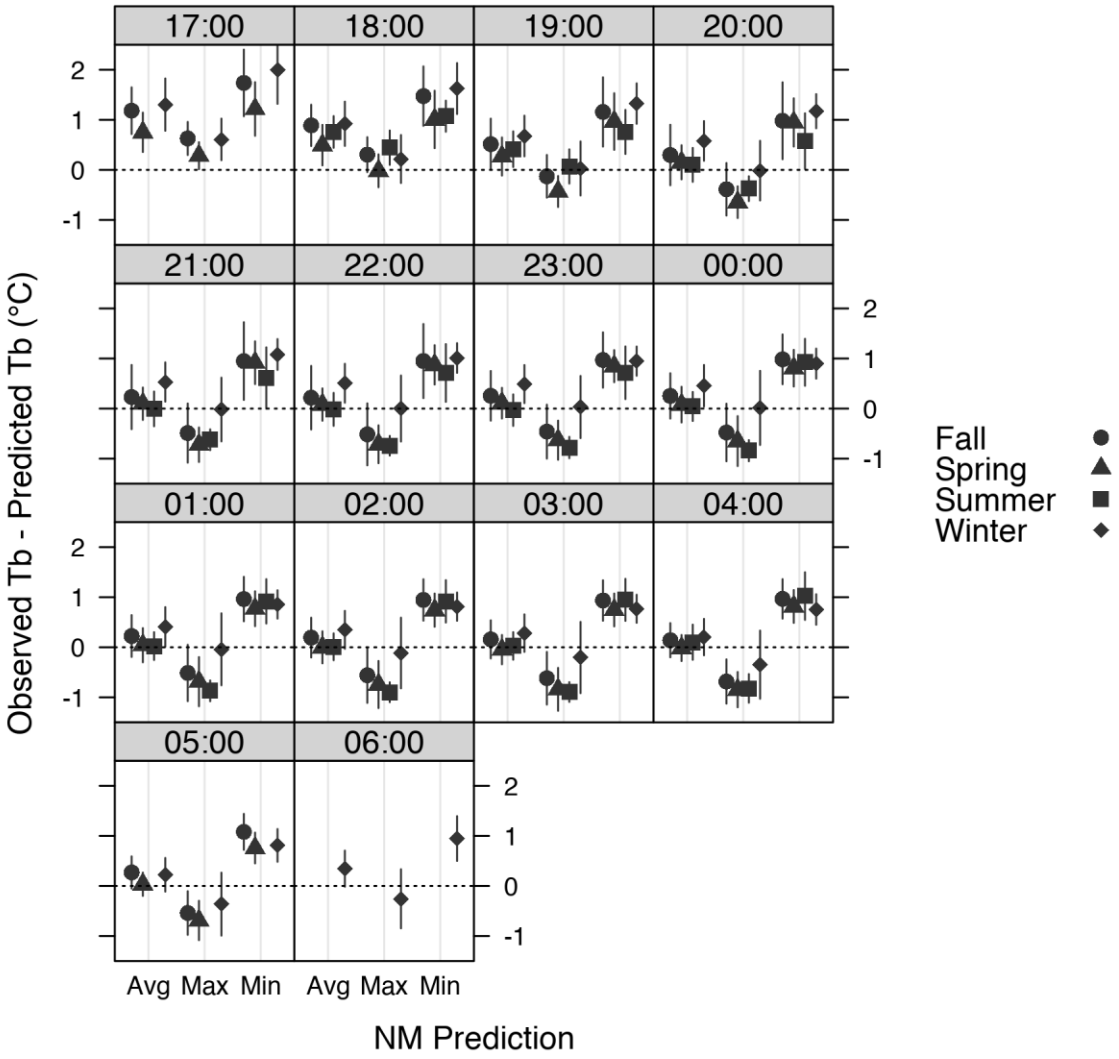
17:00
18:00
19:00
20:00
21:00
22:00
23:00
00:00
01:00
02:00
03:00
04:00
05:00
06:00
Observed Tb - Predicted Tb (°C)
Avg Max Min
Avg Max Min
NM Prediction
Fall
Spring
Summer
Winter

CRediT AUTHOR STATEMENTS

Paul D. Mathewson: Conceptualization, Methodology, Formal analysis, Software, Investigation, Data curation, Writing-Original Draft, Visualization **Warren P. Porter:** Conceptualization, Methodology, Supervision, Resources, Writing-Review & Editing **Louise Barrett:** Methodology, Investigation, Resources, Writing-Review & Editing, Supervision, Funding acquisition **Andrea Fuller:** Methodology, Investigation, Resources, Writing-Review & Editing, Supervision, Funding acquisition **S. Peter Henzi:** Methodology, Investigation, Writing-Review & Editing Supervision, Funding acquisition **Robyn S. Hetem:** Methodology, Investigation, Resources, Writing-Review & Editing Supervision, Funding acquisition **Christopher Young:** Investigation, Data Curation, Writing-Review & Editing **Richard McFarland:** Conceptualization, Methodology, Investigation, Resources, Writing-Review & Editing, Supervision, Funding acquisition